# Report about Fluidization

Presented by:

Dr. Sherko Ahmad Flamarz Al-Arkawazi Ph.D in Mechanical Engineering

Table of contents	Page
1. Introduction	1
2. Particle Characteristics	2
2.1 Particle Size	2
2.2 Particle Density	2
2.3 Particle Shape Factor	2
2.4 Particle Regime	2-3
3. Mechanism of fluidization	3-4
3.1 Minimum Fluidization Velocity	4-5
3.2 The effect of tortuosity	5
4. Particle-fluid interaction forces	5
5. Empirical results	6
<ol><li>Modeling fluidized beds</li></ol>	7
6.1 Hard-sphere approach	7
6.2 Soft-sphere approach	8
<ol><li>Modeling the fluidization process</li></ol>	8
8. Coupling DEM-CFD	8
8.1 Computational Fluid Dynamics (CFD) approach	8-9
8.2 Particle dynamics (Discrete element modelling of granular media)	9-10
9. The effective forces acting on the particles suspended in fluid	10
10. Discussion	10
11. Nomenclatures	1
12 Grands latters	2
13. References	12 12

### 1. Introduction

When a liquid or a gas is passed at very low velocity up through a bed of solid particles, the particles do not move, and the pressure drop is given by the Ergun equation. If the fluid velocity is steadily increased, the pressure drop and the drag on individual particles increase, and eventually the particles start to move and become suspended in the fluid.

The terms "fluidization" and "fluidized bed" are used to describe the condition of fully suspended particles, since the suspension behaves like a dense fluid. This is achieved by pumping a fluid, either a gas or a liquid, upwards through the bed at a rate that is sufficient to exert a force on the particles that exactly counteracts their weight; in this way, instead of a rigid structure held in place by means of gravity-derived contact forces, the bed acquires fluid-like properties, free to flow and deform, with the particles able to move relatively freely with respect to one another, figure 1 show the fluidization process.

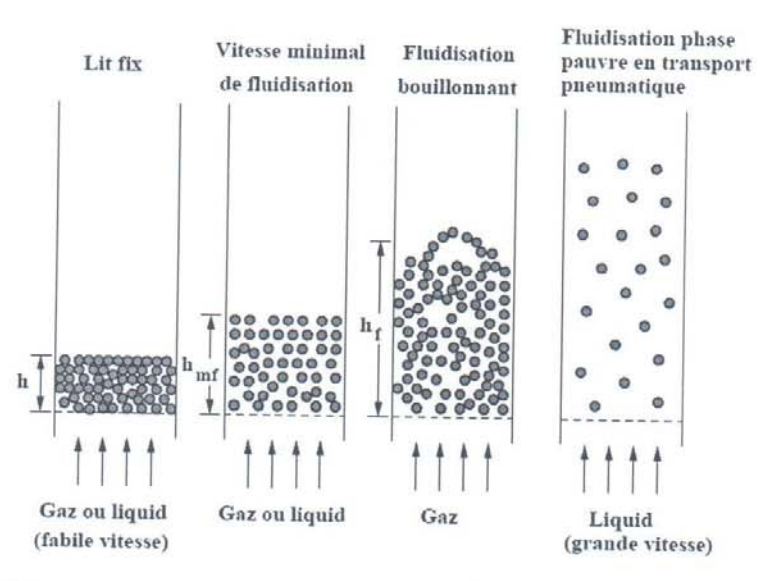


Figure 1: Fluidization process; a) fixed bed, b) minimum fluidization velocity, c) bubbling fluidization, and d) transport.

The fluidized bed is one of the best known contacting methods used in the processing industry, for instance in oil refinery plants. Among its chief advantages are that the particles are well mixed leading to low temperature gradients, they are suitable for both small and large scale operations and they allow continuous processing. Nowadays, fluidized beds are widely used in the chemical and process industries for a large variety of processes. A major application of fluidized bed technology is to be found in the catalytic-cracking reactor, which lies at the heart of the petroleum refining process. Other applications, established and potential are boundless. Gas-fluidized beds are widely used in chemical reactors, and also as combustors to raise steam for power generation. Agricultural waste and purpose-grown energy crops can be fluidized in steam to produce a hydrogen-rich fuel gas. Liquid-fluidized beds are employed extensively in water treatment, minerals processing and fermentation technology.

## 2. Particle Characteristics

The most important properties for fluidization are particle size, particle density, sphericity etc. Fluidized bed design procedures require an understanding of particle properties [1].

#### 2.1 Particle Size

The solid particles used in a fluidized bed are not identical in size and hence follow a particle size distribution. Mean particle diameter,  $d_{p}$ , is generally used for the design. When a distribution of particle sizes exits, an equation for calculating the mean diameter is

$$d_p = \frac{1}{\sum_{i} \frac{x_i}{d_{pi}}} \tag{1}$$

Where  $x_i$  is the volume fraction (or mass fraction if the particles all have the same density) of particles with diameter  $d_{pi}$ . The surface mean diameter is the most useful particle size correlation because hydrodynamic forces act at the outside surface of the particle.

#### 2.2 Particle Density

Density is a characterization factor of a mass of solids. Bulk density is a measure of the weight of assemblage of particles divided by the volume they occupy. This measurement includes the voids between the particles and the voids within the porous particles. The term solid density is the density of the solid material if it has zero porosity. Fluid bed calculations generally used the particle density,  $\rho_p$ , which is the weight of a single particle divided by its volume (including the pores).

#### 2.3 Particle Shape Factor

The shape of an individual particle is expressed in terms of the sphericity, which is independent of particle size. The sphericity,  $\varphi$ , of a particle is the ratio of the surface area of a sphere, whose volume is equal to that of the particle, divided by the actual surface area of the particle. For a non-spherical particle, the sphericity is defined as:

$$\varphi = \frac{6V_p}{d_p S_p} \tag{2}$$

For a spherical particle of diameter,  $d_p$ ,  $\varphi = 1.0$ .

## 2.4 Particle Regime

Not every particle can be fluidized. The behavior of solid particles in fluidized beds depends mostly on their size and density. A careful observation by Geldart [1, 2] is shown in figure 2 in which the characteristics of the four different powder types were categorized as follows:

• Group A is designated as 'aeratable' particles. These materials have small mean particle size  $(d_p < 30 \ \mu m)$  and/or low particle density ( $\leq 1.4 \ g/cm$ ). Fluid cracking catalysts typically are in this category. These solids fluidize easily, with smooth fluidization at low gas velocities without the formation of bubbles. At higher gas velocity, a point is eventually reached when bubbles start to form and the minimum bubbling velocity,  $U_{mb}$  is always greater than  $u_{mf}$ .

- Group B is called 'sandlike' particles and some call it bubbly particles. Most particles of this group have size 150 µm to 500 µm and density from 1.4 to 4 g/cm. For these particles, once the minimum fluidization velocity is exceeded, the excess gas appears in the form of bubbles. Bubbles in a bed of group B particles can grow to a large size. Typically used group B materials are glass beads and coarse sand.
- Group C materials are 'cohesive', or very fine powders. Their sizes are usually less than 30 μm, and they are extremely difficult to fluidize because inter particle forces are relatively large, compared to those resulting from the action of gas. In small diameter beds, group C particles easily give rise to channeling. Examples of group C materials are talc, flour and starch.
- Group D is called 'spoutable' and the materials are either very large or very dense. They are difficult to fluidize in deep beds. Unlike group B particles, as velocity increases, a jet can be formed in the bed and material may then be blown out with the jet in a spouting motion. If the gas distribution is uneven, spouting behavior and severe channeling can be expected. Roasting coffee beans, lead shot and some roasting metal ores are examples of group D materials.

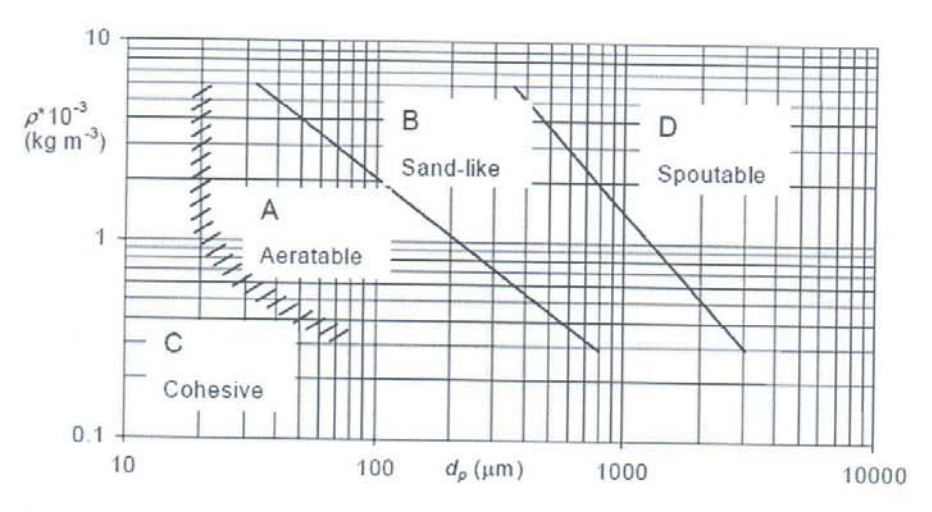


Figure 1: Diagram of the Geldart classification of particles (Geldart, 1973)

Geldart's classification is clear and easy to use as displayed in figure 1 for fluidization at ambient conditions and for u less than about  $10 \cdot u_{mf}$ . For any solid of a known density  $\rho_s$  and mean particle size  $d_p$  this graph shows the type of fluidization to be expected. It also helps predicting other properties such as bubble size, bubble velocity, the existence of slugs etc...

### 3. Mechanism of fluidization

When a fluid is admitted at the bottom of a packed bed of solids at a low flow rate, it passes upward through bed without causing any particle motion. If the particles are quite small, flow in the channels between the particles will be laminar and the pressure drop across the bed will be proportional to the superficial velocity and for turbulent situations, pressure drop across the

bed increase nonlinearly with the increase in the superficial velocity. As the velocity is gradually increased, the pressure drop increases, but particles do not move and the bed height remains the same. At a certain velocity, the pressure drop across the bed counterbalances the force of gravity on the particles or the weight of the bed, and any other further increase in velocity causes the particles to move and the true fluidization begins. For a high enough fluid velocity, the friction force is large enough to lift the particles. This represents the onset of fluidization. Once the bed is fluidized pressure drop across the bed remains constant, but the bed height continues to increase with increasing flow.

## 3.1 Minimum Fluidization Velocity

The superficial fluid velocity, at which the bed of particles is just fluidized, is normally called the minimum fluidization velocity or designated by  $u_{mf}$ . This state of incipient fluidization can be described by an equation giving the pressure drop in a fluid flowing through a packed bed, such as the so-called Ergun equation [3]:

$$\frac{\Delta P}{L} = 150 \frac{\left(1 - \varepsilon_{mf}\right)^2}{\varepsilon_{mf}^3} \frac{\mu_f u_{mf}}{\left(\phi \cdot d_p\right)^2} + 1.75 \frac{\left(1 - \varepsilon_{mf}\right) \rho_f u_{mf}^2}{\varepsilon_{mf}^3} \frac{\rho_f u_{mf}^2}{\phi \cdot d_p}$$
(3)

$$\varepsilon = 1 - \frac{m_s \rho_b}{m_b \rho_s} \tag{4}$$

Since voids are empty spaces,  $m_b = m_s$ 

$$\varepsilon = 1 - \frac{\rho_b}{\rho_s} \tag{5}$$

in which  $\Delta P$  is equal to the bed weight per unit cross-sectional area, and  $\rho_b$  is the density of the bed. When applying the Ergun equation, one has to know the minimum fluidization voidage  $\varepsilon_{mf}$ , although it is frequently an unknown. The relationship between the pressure drop in the bed  $\Delta P_B$  and the minimum fluidization velocity  $u_{mf}$  is shown in figure 3.

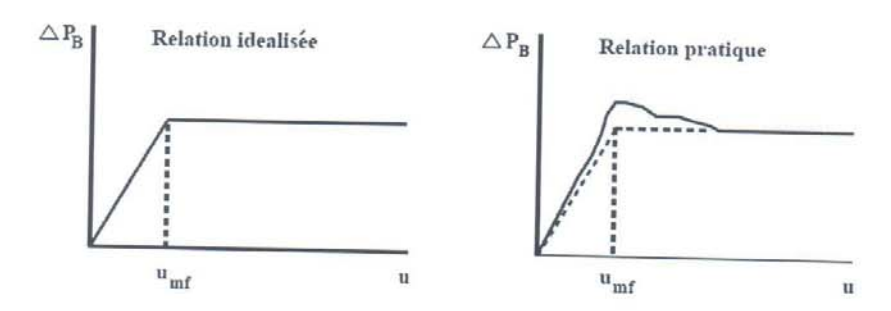


Figure 3: Unrecoverable pressure loss in a fluidized bed.

Wen and Yu (1966) [4] developed an expression for the minimum fluidization velocity for a range of particle types and sizes by assuming the following approximations to hold based on experimental data:

$$\frac{1}{\varphi^2 \varepsilon_{mf}^3} \approx 11$$
 and  $\frac{1}{\varphi \varepsilon_{mf}^3} \approx 14$  (6)

They combined these with the Ergun equation and obtained the relation:

$$Re_{mf} = \frac{d_p U_{mf} \rho_f}{\mu_f} \left( \sqrt{33.7^2 + 0.0408 \frac{d_p^3 \rho_f (\rho_s - \rho_f) g}{\mu_f^2}} - 33.7 \right)$$
 (7)

#### 3.2 The effect of tortuosity

Tortuosity is used to account for the increase in distance a diffusing molecule travels due to bending and branching of pores. Thus, the tortuosity for a porous medium is defined as the ratio of the actual path length from start to goal through the pores to the Euclidean distance (shortest linear distance).

$$T = \frac{L_{actual}}{L_{euclideam}}, T \ge 1 \tag{8}$$

which T is the tortuosity,  $L_{\text{actual}}$  the actual path length through the pores, and  $L_{\text{euclidean}}$  is the shortest distance between the start and end points in euclidean space. The trend of tortuosity (T) with porosity  $(\varepsilon)$  as shown in figure 4 is captured by the simple relation [4]:

$$T = \frac{1}{\varepsilon} \tag{9}$$

Figure 4: Tortuosity as a function of porosity

## 4. Particle-fluid interaction forces

The fluid passing through the granular medium will interact with the particles, generating different interaction forces, in addition to the buoyancy. The main interaction force is drag force, which will be the driving force of fluidization. The drag force is closely associated with the shape of the particle, the relative velocity between the particle and the fluid, and properties of particles and fluid. Two methods were used to determine the drag of a fluid force on particles. The first method is based on empirical correlations according to a drop bed pressure,

Ergun and Wen & Yu [3, 4] or a bed expansion experienced by Richardson [5]. The second method is based on direct numerical simulations (DNS) Small scale (Choi & Joseph [6]) and Lattice-Boltzmann (LB). According Feng & Yu [7], there are three patterns CFD-DEM simulation flow fluid-solid fluidized:

- Scheme 1: The force between the particles and the fluid is calculated by a local
  averaging method which is the same as that used in the two-fluid model, as the fluid
  force on each particle is calculated separately according to the speed of the particle [8,
  9].
- Scheme 2: The force between the particles and the fluid phase is first calculated to locally, as in Figure 1. This value is then distributed to the individual particles of a given rule [10, 11].
- Scheme 3: At each time step, the fluid interaction forces on the individual particles are
  calculated in a spreadsheet cell. The values are then added together to produce the
  force of fluid-particle interaction at the level of the cell [12, 13].

## 5. Empirical results

It has been widely verified that a plot of u against  $\varepsilon$  on logarithmic co-ordinates approximates closely to a straight line over the full range of bed expansion, regardless of the flow regime. The observations may therefore be described by:

$$u = u_{i} \varepsilon^{n} \tag{10}$$

where u is sedimentation velocity of a suspension of uniform particles,  $u_t$  is free falling velocity of an individual particle,  $\varepsilon^n$  is porosity function and n is index. The relation shown in equation 10 known as the Richardson-Zaki equation [14] after the authors of an extensive experimental investigation into its applicability (figure 5).

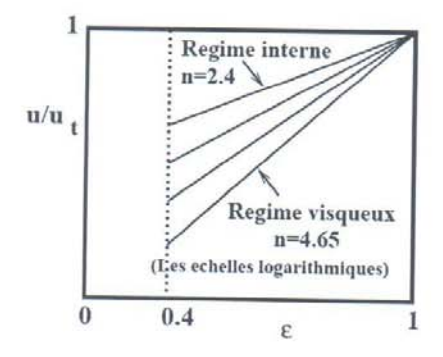


Figure 5: Steady-state expansion characteristics for homogeneous fluidization: the Richardson-Zaki relation

## 6. Modeling fluidized beds

In order to improve design and scale-up procedures of fluidized beds, a sound understanding of the transport phenomena in these systems is vital. There exists a vast amount of literature on various experimental investigations of transport phenomena in fluidized beds. With the use of computer models one is able to 'look' inside the fluidized bed without disturbing the flowfield. The computer models possess sufficient predictive capabilities; they have the additional advantage over experiments that several design options and operation conditions can be tested with relative ease. Despite these advantages, the construction of reliable models for largescale fluid-solid contactors is seriously hindered by the lack of understanding of the fundamentals of dense fluid-particle flows. In particular, the phenomena which can be related both to the effective fluid-particle interaction (drag forces), particle-particle interactions (collision forces) figure 6, and particle-wall interaction, are not well understood. The prime difficulty here is the large separation of scales: the largest flow structures can be of the order of meters; yet these structures are directly influenced by details of the particle-particle and particle-fluid interactions, which take place on the scale of millimeters, or even micrometers. To describe the hydrodynamics of the gas and particle phase, continuum-(Eulerian) and discrete-(Lagrangian) type of models have been developed. In general, there are two types of particles (spheres); hard sphere and soft sphere.

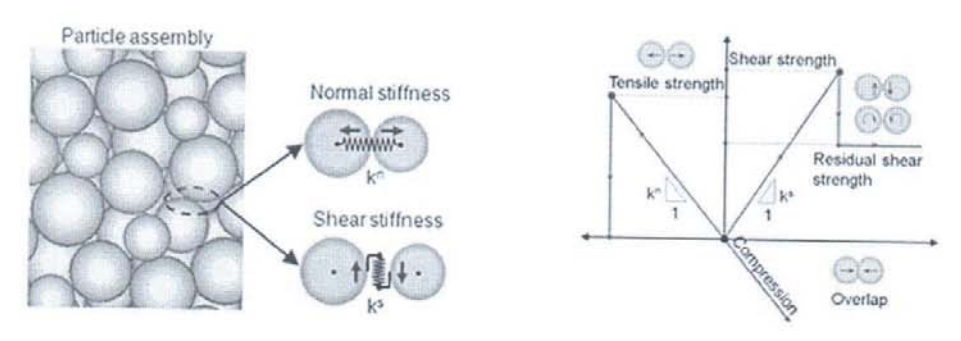


Figure 6: Particle-particle interactions (collision forces)

### 6.1 Hard-sphere approach

In a hard-sphere system the trajectories of the particles are determined by momentumconserving binary collisions. The interactions between particles are assumed to be pair-wise additive and instantaneous. In the simulation, the collisions are processed one by one according to the order in which the events occur. For not too dense systems, the hard-sphere models are considerably faster than the soft-sphere models.

At high particle number densities or low coefficients of normal restitution e, the collisions will lead to a dramatically decrease in kinetic energy. This is the so-called inelastic collapse, in which regime the collision frequencies diverge as relative velocities vanish. Clearly in that case, the hard-sphere method becomes useless.

6.2 Soft-sphere approach

In more complex situations, the particles may interact via short- or long-range forces, and the trajectories are determined by integrating the Newtonian equations of motion. The soft sphere method originally developed by Cundall and Strack (1979) [15] was the first granular dynamics simulation technique published in the open literature. Soft-sphere models use a fixed time step and consequently the particles are allowed to overlap slightly. The contact forces are subsequently calculated from the deformation history of the contact using a contact force scheme.

The soft-sphere models allow for multiple particle overlap although the net contact force is obtained from the addition of all pair-wise interactions. The soft-sphere models are essentially time driven, where the time step should be carefully chosen in the calculation of the contact forces. The soft-sphere models that can be found in literature mainly differ from each other with respect to the contact force scheme that is used. In the force scheme a continuous potential of an exponential form is used, which contains two unknown parameters: the stiffness of the interaction and an interaction constant.

## 7. Modeling the fluidization process

In the literature, two classes of models have been proposed to describe the performance of fluidized bed reactors; one based on a continuous approach and the other on an approach discrete (Zhu et al. [16]). The continuous approach, such as that of the model with two fluids, describes two phases as two immiscible fluid phases governed by equations balance (Two Fluid Model (TFM)) Gidaspow [17].

The discrete approach is based on the analysis of movement of individual particles and has the advantage of not requiring general assumptions about the behavior of solids or state of equilibrium. This approach has been proposed by Cundall and Strack [15].

#### 8. Coupling DEM-CFD

DEM-CFD simulations have to cover a huge variety of regimes [18, 19]. The physics must be described correctly where the particle motion is controlled by the fluid flow. The long term goal is to develop a DEM-CFD solver being robust and efficient enough to handle industrial granular flow applications.

## 8.1 Computational Fluid Dynamics (CFD) approach

Fluid Dynamics is the study of fluids in motion. The basic equations governing fluid motion have been known for more than 150 years and are called the Navier-Stokes equations which govern the motion of a viscous, heat conducting fluid. Various simplifications of these equations exist depending on which effects are insignificant. There are several dimensionless parameters which characterize the relative importance of various effects. Some of these are Mach number, Reynolds number and Prandtl number. Their numerical solution requires the use of the finite volume method; the latter is located in all the codes in general fluid mechanics. It is based on a co-located Finite Volume approach that accepts meshes with any type of cell for calculations of the fluid flow. The equations of Navier-Stokes for compressible and incompressible flows, with or without heat transfer and turbulence are;

The continuity equation (conservation of mass):

$$\frac{D\rho}{Dt} + \rho \nabla \cdot \vec{u} = 0 \tag{11}$$

The motion equation (conservation of momentum):

$$\rho \frac{D\bar{u}}{Dt} = -\nabla P - \nabla . \tau + \rho \bar{g} \tag{12}$$

Shear stress constitutive equation:

$$\tau = -\mu \left( \nabla u + \nabla \vec{u}^T - \frac{2}{3} \nabla \vec{u} \right) \tag{13}$$

The simplified motion equation for an incompressible Newtonian fluid with uniform viscosity

$$\rho \frac{D\vec{u}}{Dt} = -\nabla P - \mu \nabla^2 \vec{u} + \rho \vec{g} \tag{14}$$

Where t is time,  $\rho_i \vec{u}$  and p are density, velocity, and pressure of the fluid respectively,  $\tau$  is the viscous stress tensor and  $\vec{g}$  refers to gravity.

# 8.2 Particle dynamics (Discrete element modelling of granular media)

The most general method of discrete elements is used to model real deformable particles and complex forms (from the ellipsoid to the polygon). For simple case it consider as spherical non-deformable and non-penetrable. Discrete Element Method provides coordinates, speed and reactions of contact of each particle at each time step.

Two parameters defining particle to particle and particle to wall interactions are introduced. First parameter is the coefficient of normal restitution; Second parameter is the coefficient of dynamic friction, which arises in collisions involving sliding. The particles are tracked individually by the Newton's second law of motion. Each particle has two types of motion, translational and rotational motions. The motion of each individual particle is governed by the laws of conservation of linear momentum (Newton's second law of motion) and angular momentum in two dimensions, expressed, for the *i*-particle, by:

$$m_i \frac{d\vec{v}_i}{dt} = m_i \vec{g} + \vec{F}_{C,i} + \vec{F}_{D,i} + \vec{F}_{B,i}$$

$$\tag{15}$$

$$I\frac{d\vec{\omega}}{dt} = \vec{T}_p \tag{16}$$

Where  $m_i$ ,  $\vec{v}_i$  represent, mass, velocity of the (i th) particle respectively,  $\vec{g}$  is acceleration due to gravity  $\vec{F}_{C,i}$  is the vector of contact forces (normal force and tangential force) between the particles,  $\vec{F}_{D,i}$  is the drag force,  $\vec{F}_{B,i}$  is buoyant force,  $I_p$  and  $\vec{\omega}$  are the moment of inertia and angular velocity of a particle,  $\vec{T}_p$  is the torque arising from the tangential components of the contact force. The fluid-solid interaction force, or drag force  $\vec{F}_{D,i}$  is determined at each particle. The drag force depends on not only the relative velocity between the solid particle

and fluid but also the presence of neighboring particles, i.e., local volume fraction of solid phase.

# 9. The effective forces acting on the particles suspended in fluid medium

A good prediction of fluidization stability requires a priori knowledge of the effective forces acting on the particles suspended in the fluid medium. The effective forces acting on a particle placed into an infinite and viscous fluid it experiences are; gravity force, buoyant force, and drag force. The gravity force is a constant and acts in the downward direction, and the buoyant force is also a constant but acts in the upward direction. The drag force, however, acts against the direction of motion and is a function of the relative velocity between the particle and liquid.

Thus according to the condition of equilibrium state;

$$\sum F_{y} = m_{i} \vec{g} \cdot \vec{i} + \vec{F}_{D,i} \cdot \vec{i} + \vec{F}_{B,i} \cdot \vec{i} = 0$$

$$\tag{17}$$

Thus for a single spherical particle:

$$\frac{\pi}{6}d_{p}^{3}\rho_{p}g = \frac{C_{D}}{8}\pi\rho_{f}d_{p}^{2}|v_{f} - v_{i}|^{2}\varepsilon^{2} + \frac{\pi}{6}d_{p}^{3}\rho_{f}g$$
(18)

Where  $\vec{i}$  is unit vector and its direction is opposite of the direction of acceleration due to gravity,  $\rho_p$  represent the density of the particle. The interaction between a single particle and fluid can be clearly distinguished and correlated for a wide range of Reynolds number (Re). However, when the processes involve multiple particle system with a varying particulate assemblage, the mathematical expressions for these systems become difficult due to the complex nature of fluid flow.

#### 10. Discussion

In this report we introduce the fluidization process and the characteristics and various regimes and schemes for the particles. Then we reviewed the literature theoretical and empirical dealing fluidization. In other part, we detailed the numerical techniques and methods that used in the simulation of the fluidization process (figure 7). Although relatively provided, we see that many issues remain unresolved, and that the authors are struggling to agree on general correlations that would apply to a wide variety of situations.

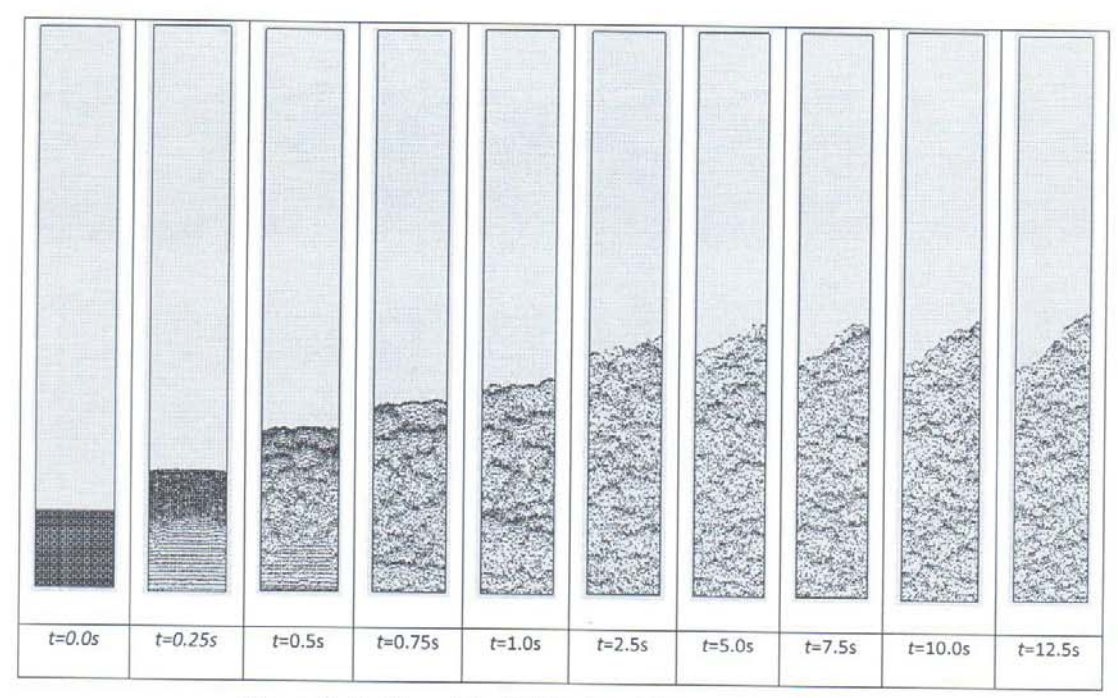


Figure 7: Position of the fluidized particles over time.

## Nomenclatures

```
C_{D,p} particle drag force coefficient
```

d<sub>p</sub> particle diameter (m)

 $\vec{F}_{C,p}$  contact force (N)

 $\vec{F}_{D,p}$  drag force (N)

 $\vec{F}_{B,p}$  buoyant force (N)

 $\vec{g}$  acceleration due to gravity (m.s<sup>-2</sup>)

 $\vec{i}$  unit vector

p pressure (Nm-2)

Rep Reynolds number

t time (s)

- $\vec{T}_p$  torque of the particle (N.m)
- T tortuosity
- $\vec{v}$  velocity vector (m.s<sup>-1</sup>)
- $\vec{v}_f$  fluid velocity vector (m.s<sup>-1</sup>)
- $I_p$  moment of inertia of a particle (kg·m<sup>2</sup>.rad-<sup>2</sup>)
- $\vec{\omega}$  angular velocity of a particle (rad.s<sup>-1</sup>)
- $m_p$  mass of (p th) particle (kg)

#### Greek letters

- τ viscous stress tensor (Pa)
- $\varepsilon_f$  porosity
- $\mu_f$  fluid viscosity (Pa.s)
- $\rho_f$  fluid density (kg.m<sup>-3</sup>)
- $\rho_p$  particle density (kg. m<sup>-3</sup>)

## References

- [1] D. Geldart. Homogenous fluidization in fine powder using various gases and pressures. *Powder Technology*, Vol. 19:133–136, 1978.
- [2] D. Geldart. Types of gas fluidization. Powder Technology, Vol. 7:285-292, 1973.
- [3] S. Ergun. Fluid flow through packed columns. Chemical Engineering and Processing, Vol. 48: 89–94, 1952.
- [4] C. Y. Wen and Y. H. Yu. Mechanics of fluidization. Chem. Engrg. Progress Symp. Series, Vol. 62, No. 62: 100–111, 1966.
- [5] J. F. Richardson. Incipient fluidization and particulate systems. In: Fluidization. Academic Press, New York., 1971.
- [6] H. G. Choi and D. D. Joseph. Fluidization by lift of 300 circular particles in plane poiseuille flow by direct numerical simulation. *Journal of Fluid Mechanics*, Vol. 438: 101–128, 2001.
- [7] Y. Q. Feng and A. B. Yu. Assessment of model formulations in the discrete particle simulation of gas-solid flow. *Industrial and Engineering Chemistry Research*, Vol. 43: 8378–8390, 2004a.
- [8] B. P. B. Hoomans, J. A. M. Kuipers, W. J. Briels, and W. P. M. van Swaaij. Discrete particle simulation of bubble and slug formation in a two-dimensional gas-fluidized bed.
- [9] Y. Tsuji, T. Kawaguchi, and T. Tanaka. Discrete particle simulation of 2-dimensional fluidized-bed. *Powder Technology*, Vol. 77: 79–87, 1993.

- [10] T. Mikami, H. H. Kamiya, and M. Horio. Numerical simulation of cohesive powder behavior in a fluidized bed. *Chemical Engineering Science*, Vol. 53: 1927–1940, 1998.
- [11] D. G. Rong, T. Mikami, and M. Horio. Particle and bubble movements around tubes immersed in fluidized beds-a numerical study. *Chemical Engineering Science*, Vol. 54: 5737–5754, 1999.
- [12] B. H. Xu and A. B. Yu. Numerical simulation of the gas-solid flow in a fluidized bed by combining discrete particle method with computational fluid dynamics. *Chemical Engineering Science*, Vol. 52: 2785–2809, 1997.
- [13] Y. Q. Feng and A. B. Yu. Assessment of model formulations in the discrete particle simulation of gas-solid flow. *Industrial and Engineering Chemistry Research*, Vol. 43: 8378–8390, 2004a.
- [14] Richardson, J. F., & Zaki, W. N. Sedimentation and fluidization: Part I. Transaction Institute of Chemical Engineers 1954, 32, 35–53.
- [15] Cundall, P.A; Strack, O.D.L. A discrete numerical model for granular assemblies. Geotechnique 1979, 29, pp 47–65.
- [16] H. P. Zhu, Z. Y. Zhou, R. Y. Yang, and A. B. Yu. Discrete particle simulation of particulate systems: Theoretical developments. *Chemical Engineering Science*, Vol. 62: 3378–3396, 2007.
- [17] D. Gidaspow. Multiphase flow and fluidization. Technical report, Academic Press, San Diego., 1994.
- [18] S. Al-Arkawazi, C. Marie, K. Benhabib, and P. Coorevits. Modeling the behavior of a fluidized bed by coupling DEM-CFD. In 20 th International Congress of Chemical and Process Engineering, CHISA 25-29 August, Prague, Czech Republic, 2012.
- [19] S. AL-ARKAWAZI. Modeling the interactions between fluid-granular medium by coupling CFD DEM, including heat transfer. PhD thesis, Sciences, Technologies et Santé, University of Picardie Jules Verne, Mars 2014.